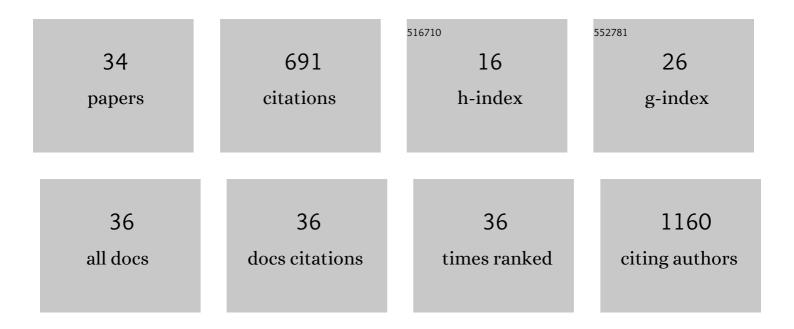
Mika Valden

List of Publications by Year in descending order

Source: https://exaly.com/author-pdf/7034223/publications.pdf Version: 2024-02-01



Μικά Πλισέν

#	Article	IF	CITATIONS
1	Tunable Ti ³⁺ -Mediated Charge Carrier Dynamics of Atomic Layer Deposition-Grown Amorphous TiO ₂ . Journal of Physical Chemistry C, 2022, 126, 4542-4554.	3.1	25
2	GaAs surface passivation for InAs/GaAs quantum dot based nanophotonic devices. Nanotechnology, 2021, 32, 130001.	2.6	7
3	Manganese Doping Promotes the Synthesis of Bismuthâ€based Perovskite Nanocrystals While Tuning Their Band Structures. Small, 2021, 17, e2100101.	10.0	25
4	Ultrathinâ€Walled 3D Inorganic Nanostructured Networks Templated from Crossâ€Linked Cellulose Nanocrystal Aerogels. Advanced Materials Interfaces, 2021, 8, 2001181.	3.7	2
5	Perovskite Nanocrystals: Manganese Doping Promotes the Synthesis of Bismuthâ€based Perovskite Nanocrystals While Tuning Their Band Structures (Small 19/2021). Small, 2021, 17, 2170089.	10.0	1
6	Performance and characterization of the FinEstBeAMS beamline at the MAXÂIV Laboratory. Journal of Synchrotron Radiation, 2021, 28, 1620-1630.	2.4	28
7	Interface Engineering of TiO ₂ Photoelectrode Coatings Grown by Atomic Layer Deposition on Silicon. ACS Omega, 2021, 6, 27501-27509.	3.5	11
8	Optimization of Photogenerated Charge Carrier Lifetimes in ALD Grown TiO2 for Photonic Applications. Nanomaterials, 2020, 10, 1567.	4.1	20
9	Bâ€Site Coâ€Alloying with Germanium Improves the Efficiency and Stability of Allâ€Inorganic Tinâ€Based Perovskite Nanocrystal Solar Cells. Angewandte Chemie, 2020, 132, 22301-22309.	2.0	10
10	Bâ€Site Coâ€Alloying with Germanium Improves the Efficiency and Stability of Allâ€Inorganic Tinâ€Based Perovskite Nanocrystal Solar Cells. Angewandte Chemie - International Edition, 2020, 59, 22117-22125.	13.8	75
11	Modification of Surface States of Hematite-Based Photoanodes by Submonolayer of TiO ₂ for Enhanced Solar Water Splitting. Journal of Physical Chemistry C, 2020, 124, 13094-13101.	3.1	18
12	Gas-phase endstation of electron, ion and coincidence spectroscopies for diluted samples at the FinEstBeAMS beamline of the MAXâ€IV 1.5â€GeV storage ring. Journal of Synchrotron Radiation, 2020, 27, 1080-1091.	2.4	19
13	Large-scale efficient water harvesting using bioinspired micro-patterned copper oxide nanoneedle surfaces and guided droplet transport. Nanoscale Advances, 2019, 1, 4025-4040.	4.6	33
14	Chemical Dissolution of Pt(111) during Potential Cycling under Negative pH Conditions Studied by Operando X-ray Photoelectron Spectroscopy. Journal of Physical Chemistry C, 2019, 123, 25128-25134.	3.1	19
15	Charge carrier dynamics in tantalum oxide overlayered and tantalum doped hematite photoanodes. Journal of Materials Chemistry A, 2019, 7, 3206-3215.	10.3	25
16	Diversity of TiO ₂ : Controlling the Molecular and Electronic Structure of Atomic-Layer-Deposited Black TiO ₂ . ACS Applied Materials & Interfaces, 2019, 11, 2758-2762.	8.0	38
17	Fabrication of ultrathin multilayered superomniphobic nanocoatings by liquid flame spray, atomic layer deposition and silanization. Nanotechnology, 2018, 29, 185708.	2.6	2
18	Improved Stability of Atomic Layer Deposited Amorphous TiO ₂ Photoelectrode Coatings by Thermally Induced Oxygen Defects. Chemistry of Materials, 2018, 30, 1199-1208.	6.7	81

Mika Valden

#	Article	IF	CITATIONS
19	The role of (FeCrSi)2(MoNb)-type Laves phase on the formation of Mn-rich protective oxide scale on ferritic stainless steel. Corrosion Science, 2018, 132, 214-222.	6.6	21
20	Reversible Photodoping of TiO ₂ Nanoparticles for Photochromic Applications. Chemistry of Materials, 2018, 30, 8968-8974.	6.7	69
21	Design aspects of all atomic layer deposited TiO ₂ –Fe ₂ O ₃ scaffold-absorber photoanodes for water splitting. Sustainable Energy and Fuels, 2018, 2, 2124-2130.	4.9	7
22	Building Up Colors: Multilayered Arrays of Peryleneimides on Flat Surfaces and Mesoporous Layers. ChemPlusChem, 2017, 82, 705-715.	2.8	0
23	Tailored Fabrication of Transferable and Hollow Weblike Titanium Dioxide Structures. ChemPhysChem, 2017, 18, 64-71.	2.1	4
24	Improved Corrosion Properties of Hot Dip Galvanized Steel by Nanomolecular Silane Layers as Hybrid Interface Between Zinc and Top Coatings. Corrosion, 2017, 73, 169-180.	1.1	6
25	Grain orientation dependent Nb–Ti microalloying mediated surface segregation on ferritic stainless steel. Corrosion Science, 2016, 112, 204-213.	6.6	16
26	Improved antifouling properties and selective biofunctionalization of stainless steel by employing heterobifunctional silane-polyethylene glycol overlayers and avidin-biotin technology. Scientific Reports, 2016, 6, 29324.	3.3	21
27	Color Bricks: Building Highly Organized and Strongly Absorbing Multicomponent Arrays of Terpyridyl Perylenes on Metal Oxide Surfaces. Chemistry - A European Journal, 2016, 22, 1501-1510.	3.3	4
28	Ormocomp-Modified Glass Increases Collagen Binding and Promotes the Adherence and Maturation of Human Embryonic Stem Cell-Derived Retinal Pigment Epithelial Cells. Langmuir, 2014, 30, 14555-14565.	3.5	23
29	Biofunctional hybrid materials: bimolecular organosilane monolayers on FeCr alloys. Nanotechnology, 2014, 25, 435603.	2.6	6
30	Effect of plasma treated Ag/indium tin oxide anode modification on stability of polymer solar cells. Solar Energy Materials and Solar Cells, 2014, 128, 330-334.	6.2	7
31	Controlling the synergetic effects in (3-aminopropyl) trimethoxysilane and (3-mercaptopropyl) trimethoxysilane coadsorption on stainless steel surfaces. Applied Surface Science, 2014, 317, 856-866.	6.1	14
32	Characterization of silane layers on modified stainless steel surfaces and related stainless steel–plastic hybrids. Applied Surface Science, 2011, 257, 9335-9346.	6.1	39
33	Ag/Cu(100) Surface Alloy and Polycrystalline Cu(Ag) Alloy Studied by XPS. Surface Science Spectra, 2008, 15, 31-40.	1.3	2
34	Rh oxide reducibility and catalytic activity of model Pt–Rh catalysts. Catalysis Today, 2005, 100, 327-330.	4.4	13